

# ATPase Activity of *Escherichia coli* Rep Helicase Is Dramatically Dependent on DNA Ligation and Protein Oligomeric States<sup>†</sup>

Isaac Wong, Keith J. M. Moore, Keith P. Bjornson, John Hsieh, and Timothy M. Lohman\*

Department of Biochemistry and Molecular Biophysics, Washington University School of Medicine, 660 South Euclid Avenue, Box 8231, St. Louis, Missouri 63110

Received December 15, 1995; Revised Manuscript Received February 9, 1996<sup>⊗</sup>

**ABSTRACT:** The *Escherichia coli* Rep helicase catalyzes the unwinding of duplex DNA using the energy derived from ATP binding and hydrolysis. Rep functions as a dimer but assembles to its active dimeric form only on binding DNA. Each protomer of a dimer contains a DNA binding site that can bind either single-stranded (S) or duplex (D) DNA. The dimer can bind up to two oligodeoxynucleotides in five DNA-ligation states: two half-ligated states, P<sub>2</sub>S and P<sub>2</sub>D, and three fully-ligated states, P<sub>2</sub>S<sub>2</sub>, P<sub>2</sub>D<sub>2</sub>, and P<sub>2</sub>SD. We have previously shown that the relative stabilities of these ligation states are allosterically regulated by the binding and hydrolysis of ATP and have proposed an “active rolling” model for DNA unwinding where the enzyme cycles through a series of these ligation states in a process that is coupled to the catalytic cycle of ATP hydrolysis [Wong, I., & Lohman, T. M., (1992) *Science* 256, 350–355]. The basal ATPase activity of Rep protein is stimulated by ss DNA binding and by protein dimerization. We have measured the steady-state ATPase activities of Rep bound to dT(pT)<sub>15</sub> in each distinct ss DNA ligation state (PS, P<sub>2</sub>S, and P<sub>2</sub>S<sub>2</sub>) to compare with our previous measurements with unligated Rep monomer (P) [Moore, K. J. M., & Lohman, T. M. (1994) *Biochemistry* 33, 14550]. We find the ATPase activity of Rep is influenced dramatically by both dimerization and ss DNA ligation state, with the following *k*<sub>cat</sub> values for ATP hydrolysis increasing by over 4 orders of magnitude: 2.1 × 10<sup>−3</sup> s<sup>−1</sup> for P, 2.17 ± 0.04 s<sup>−1</sup> for PS, 16.5 ± 0.2 s<sup>−1</sup> for P<sub>2</sub>S, and 71 ± 2.5 s<sup>−1</sup> for P<sub>2</sub>S<sub>2</sub> (20 mM Tris-HCl, pH 7.5, 6 mM NaCl, 5 mM MgCl<sub>2</sub>, 10% glycerol, 4 °C). The apparent *K*<sub>M</sub>'s for ATP hydrolysis are 2.05 ± 0.1 μM for PS and 2.7 ± 0.2 μM for P<sub>2</sub>S. These widely different ATPase activities reflect the allosteric effects of DNA ligation and demonstrate that cooperative communication occurs between the ATP and DNA sites of both subunits of the Rep dimer. These results further emphasize the need to explicitly consider the population distribution of oligomerization and DNA ligation states of the helicase when attempting to infer information about elementary processes such as helicase translocation based solely on macroscopic steady-state ATPase measurements.

DNA helicases are motor proteins that convert the chemical energy derived from the binding and hydrolysis of nucleoside triphosphates to perform the physical work of unwinding the complementary strands of duplex DNA (Matson & Kaiser-Rogers, 1990; Lohman, 1992, 1993; Moore & Lohman, 1995; Lohman & Bjornson, 1996). These enzymes appear to be ubiquitous and provide essential functions in all DNA metabolic processes such as DNA replication, repair, and recombination (Matson et al., 1994) as well as the coupling of DNA repair to transcription (Hanawalt, 1994). However, relatively little is known about the mechanism by which this essential class of enzymes is able to utilize chemical energy to perform mechanical physical work. Although it is likely that different helicases unwind DNA by different mechanisms, they appear to share a common structural feature in that all helicases for which the assembly state has been characterized in detail are known to form oligomers, typically dimers or hexamers (Lohman,

1992, 1993; Wong et al., 1992; Lohman & Bjornson, 1996). Oligomeric structures would necessarily provide the functional helicase with the multiple DNA and nucleoside triphosphate binding sites necessary to carry out processive cycles of unwinding (Lohman, 1992; Wong et al., 1992; Wong & Lohman, 1992).

The *Escherichia coli* rep gene product, a protein with a monomer molecular weight of 76 400 (673 amino acids), was one of the first proteins to be identified and characterized as a DNA helicase (Lane & Denhardt, 1974, 1975a,b; Scott et al., 1977; Yarranton & Geftter, 1979; Kornberg et al., 1978; Arai & Kornberg, 1981; Arai et al., 1981), and is one of the few that has been studied at a mechanistic level (Chao & Lohman, 1991; Wong et al., 1992; Wong & Lohman, 1992; Amaratunga & Lohman, 1993; Moore & Lohman, 1994a,b, 1995; Bjornson et al., 1994, 1996). The *E. coli* Rep protein has been implicated in DNA replication (Lane & Denhardt, 1974, 1975a,b; Colasanti & Denhardt, 1987) as well as in DNA repair and recombination (Calendar et al., 1970; Bridges & von Wright, 1981). In the absence of DNA it exists in solution as a monomer up to its solubility limit (Chao & Lohman, 1991). However, upon binding DNA the Rep monomer is induced to assemble to its functionally active dimeric form with high affinity (*L*<sub>2S</sub> = 1–2 × 10<sup>8</sup>

<sup>†</sup> Supported by grants from the National Institutes of Health (GM 45948) and the American Cancer Society (NP-756B). I.W. and K.J.M.M. received support from an American Cancer Society Postdoctoral Fellowship (PF-3671) and a William Keck Postdoctoral Fellowship, respectively, and K.P.B. received partial support from an NIH training grant (5 T32 GM08492).

\* Author to whom correspondence should be addressed.

<sup>⊗</sup> Abstract published in *Advance ACS Abstracts*, May 1, 1996.

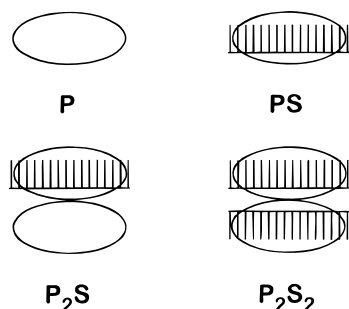


FIGURE 1: ss-DNA-ligation states of Rep. The four experimentally accessible ligation states of Rep bound to ss-DNA are shown: the free monomer, P, the ligated monomer, PS, the half-ligated dimer,  $P_2S$ , and the fully-ligated dimer,  $P_2S_2$ . Although formally possible, the unligated dimer,  $P_2$ , is not populated under experimental conditions.

$M^{-1}$ ) (Chao & Lohman, 1991; Wong et al., 1992; Wong & Lohman, 1992; Bjornson et al., 1996). Each subunit of the dimer possesses a DNA (Wong et al., 1992) and an ATP (Moore & Lohman, 1994a,b) binding site, and both subunits of the dimer can bind either single-stranded (ss) DNA or double-stranded (ds) DNA competitively (Wong et al., 1992). Thus, for a single conformation of DNA, e.g. ss-DNA (S), there are four experimentally accessible ligation states: the free monomer, P,<sup>1</sup> the DNA-bound monomer, PS, the half-ligated dimer,  $P_2S$ , and the fully-ligated dimer,  $P_2S_2$ , as shown in Figure 1. However, the Rep dimer is also capable of binding ss-DNA and ds-DNA simultaneously, one to each subunit. DNA binds with negative cooperativity to the second subunit of the Rep dimer, and this cooperativity is influenced by the conformation of DNA (ss or ds) bound to the first subunit and is further regulated allosterically by the binding of nucleotide cofactors (ATP, ADP, or AMPPNP) (Wong & Lohman, 1992).

These observations have previously led us to propose an "active rolling" mechanism for DNA unwinding by the Rep dimer (Wong & Lohman, 1992), and this mechanism has been supported by recent studies of the kinetics of Rep-catalyzed DNA unwinding (Amaratunga & Lohman, 1993; Bjornson et al., 1994). Salient features of this model are (1) at least one of the two subunits of the Rep dimer is always bound to ss-DNA to form a  $P_2S$  complex, although not always the same subunit, (2) ATP binding drives net translocation of the Rep dimer by promoting binding of the unfilled subunit of the Rep dimer to the duplex region just ahead of the unwinding fork to form Rep dimer with one subunit bound to ss-DNA and the other subunit bound to duplex DNA (a  $P_2SD$  complex), (3) ATP hydrolysis is coupled to the destabilization of multiple base pairs in the duplex region bound to Rep leading to the "melting" of that region of duplex and, displacement of the 5' ss-DNA and transient formation of a Rep dimer with both subunits bound to ss-DNA (a  $P_2S_2$  complex), the ligation state preferred in the presence of ADP, and (4) Release of the ADP and ss-DNA from one subunit returns the dimer to the starting  $P_2S$  state. A critical aspect of this model lies in the coupling of

the ATPase catalytic cycle to a series of DNA ligation state changes. To test this model, therefore, would require a detailed understanding of the kinetics and the mechanism of DNA binding, ATP binding, and hydrolysis as well as DNA unwinding. Toward this end, Moore and Lohman (1994a,b) have determined the kinetic mechanism of nucleotide binding and hydrolysis by the unligated Rep monomer, and Bjornson et al. (1996) have determined the kinetic mechanism of ss-DNA binding and ss-DNA induced Rep dimerization, both using fluorescent stopped-flow methods. In this report we have extended these studies to include measurements of the steady-state ATPase properties of all ss-DNA ligation states of Rep, namely, PS,  $P_2S$ , and  $P_2S_2$ . Our findings indicate that the ATPase activity of Rep is allosterically regulated by both DNA binding and protein dimerization in a dramatic fashion. These results also suggest caution in drawing mechanistic conclusions based solely on observed ATPase activities.

## MATERIALS AND METHODS

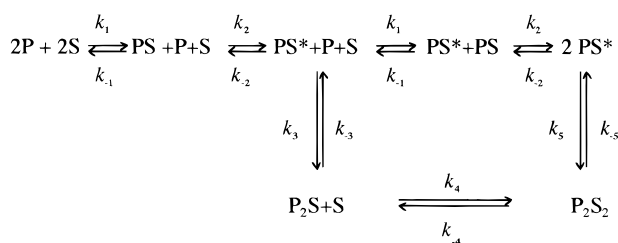
**Reagents and Buffers.** [ $\alpha$ -<sup>32</sup>P]ATP (3000 Ci/mmol) was from Amersham, U.K. Spectrophotometric grade glycerol, HPLC grade methanol, and 99% triethylamine were from Aldrich (Milwaukee, MI). All solutions were made with reagent grade chemicals, except as noted above, using Milli-Q H<sub>2</sub>O, i.e., distilled H<sub>2</sub>O that was deionized using a Milli-Q Water Purification System (Millipore Corporation, Bedford, MA). All ATPase assays were carried out in binding buffer with Mg (BBM) which contained 20 mM Tris-HCl, pH 7.5, at 4 °C, 6 mM NaCl, 5 mM MgCl<sub>2</sub>, and 10% (v/v) glycerol. Kinase buffer is 50 mM Tris-HCl, pH 7.5, at 25 °C, 10 mM MgCl<sub>2</sub>, and 10 mM 2-mercaptoethanol.

**Proteins, Enzymes, and Oligodeoxynucleotides.** *E. coli* Rep protein was purified from *E. coli* MZ-1/pRepO (Colasanti & Denhardt, 1987) to >99% purity as described (Lohman et al., 1989). Rep concentration was determined spectrophotometrically using an extinction coefficient for Rep monomer of  $\epsilon_{280} = 7.68 \times 10^4 \text{ M}^{-1} \text{ cm}^{-1}$  (Amaratunga & Lohman, 1993). T4 polynucleotide kinase was from US Biochemical Corp. (Cleveland, OH). Oligodeoxynucleotide, dT(pT)<sub>15</sub>, was synthesized using an ABI Model 391 DNA Synthesizer (Applied Biosystems Inc., Foster City, CA) and further purified to >99% purity by HPLC as described (Lohman & Bujalowski, 1988) and dialyzed (Spectra/Por 7 MWCO 1000) vs Milli-Q H<sub>2</sub>O for storage. The purity of the DNA was determined by denaturing polyacrylamide gel electrophoresis (PAGE) as described (Wong et al., 1992), and concentrations were determined spectrophotometrically in 10 mM Tris-HCl, pH 7.5, 1 mM EDTA, and 150 mM NaCl at 25 °C using an extinction coefficient of  $\epsilon_{260} = 1.29 \times 10^5 \text{ M}^{-1} \text{ cm}^{-1}$  per molecule. Poly(dT) was obtained from Midland Certified Reagent Company (Midland, TX) and its concentration determined using  $\epsilon_{260} = 8.1 \times 10^3 \text{ M}^{-1} \text{ cm}^{-1}$  per nucleotide.

**ATPase Activity.** Steady-state ATPase activity was determined by measuring the initial rate of conversion of ATP to ADP using [ $\alpha$ -<sup>32</sup>P]ATP. Reactions were initiated by addition of 1 volume (typically 10  $\mu$ L) of 10 mM ATP solution to 9 volumes (typically 90  $\mu$ L) of protein solution. At regular time intervals, aliquots were removed and quenched by mixing with an equal volume of 0.5 M EDTA. Intervals between time points ranged from 5 to 20 s

<sup>1</sup> Our nomenclature for Rep-ss DNA species is as follows: P, unligated Rep monomer; PS, Rep monomer bound to single-stranded DNA;  $P_2S$ , Rep dimer with ss DNA (S) bound to one subunit;  $P_2S_2$ , Rep dimer with ss DNA bound to both subunits;  $P_2SD$ , Rep dimer with one subunit bound to ss DNA and the other subunit bound to double stranded DNA (D).

## Scheme 1



depending on the anticipated rate of ATP hydrolysis. Eight to ten time points were taken per assay, but only the linear portion of the time course, typically corresponding to less than 60% product formation, was used to determine initial velocities. All ATPase assays were carried out at 4 °C in BBM buffer as defined above. The extent of product formation at each time point was monitored by spotting 1  $\mu$ L samples onto polyethyleneimine(PEI)-cellulose TLC plates (E. Merck, Darmstadt, Germany) which were developed using 0.3 M potassium phosphate, pH 7.0, as the mobile phase. TLC plates were then dried using a heat gun and analyzed quantitatively using a Betascope 603 (Betagen, Waltham, MA) direct beta-emission imager. Spots corresponding to radiolabeled ATP and ADP were quantitated using software supplied by the manufacturer.

**Kinetics of Transient Formation of  $P_2S_2$ .** For the experiments measuring the transient formation of  $P_2S_2$  and its ATPase activity, 75  $\mu$ L of a Rep sample (2.0 or 1.0  $\mu$ M) was preincubated with dT(pT)<sub>15</sub> (1.2 or 0.6  $\mu$ M) for 20 min at 4 °C to form  $P_2S$ . At  $t = 0$ , an additional 75  $\mu$ L of dT(pT)<sub>15</sub> at 200, 100, 50, 25, or 12.5  $\mu$ M was then added. At 20 s intervals, 10  $\mu$ L aliquots were removed and immediately mixed with 10  $\mu$ L of 2  $\mu$ M ATP and allowed to incubate for 7.5 s. A 10  $\mu$ L aliquot of this solution was then transferred into 10  $\mu$ L of 0.5 M EDTA to quench the reaction. In this experiment, the time courses of ATP hydrolysis were not linear beyond 10 s. However, we have verified that the rate of ATP hydrolysis was constant within the first 10 s of the reaction. The resulting time dependencies of the steady-state ATPase were analyzed according to the model shown in Scheme 1 using FITSIM (Zimmerle & Frieden, 1989) to obtain fitted values for  $k_4$ , the bimolecular association rate constant for dT(pT)<sub>15</sub> binding to  $P_2S$ ,  $k_5$ , the bimolecular association rate constant for 2  $PS^*$  dimerizing to form  $P_2S_2$ , and  $k_5$ , the rate constant for dissociation of  $P_2S_2$  to form 2  $PS^*$ . Because FITSIM does not allow output factors, in this case values for  $k_{cat}$ , to be floated, the best fit value of  $k_{cat}$  for  $P_2S_2$  was obtained by executing fits using different values of  $k_{cat}$  for  $P_2S_2$  and manually minimizing the sums of squares of the residuals.

**Data Analysis.** KINSIM (Barshop et al., 1983) and FITSIM (Zimmerle & Frieden, 1989) were executed on an IBM PS/2 Model 76. All other data analysis was performed using Kaleidagraph (Synergy Software, Reading, PA) on an Apple Macintosh Quadra 700 or an Apple Power Macintosh 7100/80AV.

## RESULTS

**Optimization of Rep and DNA Concentrations for Exclusive Formation of  $PS$  and  $P_2S$ .** In order to examine the ATPase activity of the individual Rep monomer and dimer species in each ss DNA ligation state,  $PS$ ,  $P_2S$ , and  $P_2S_2$ , we

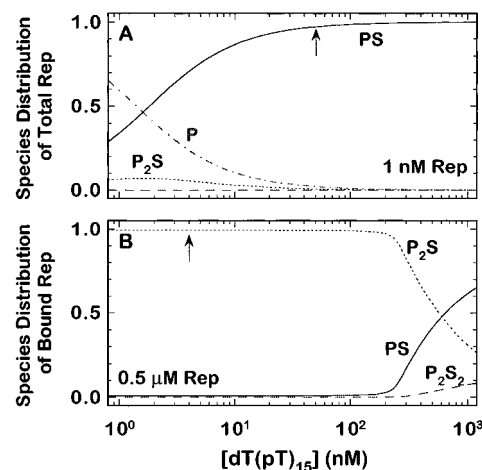


FIGURE 2: Population distribution of the ss-DNA-ligation states of Rep. The population distribution of the four Rep species ( $P$ ,  $PS$ ,  $P_2S$ , and  $P_2S_2$ ) at (A) 1 nM and (B) 0.5  $\mu$ M total Rep monomers were simulated as a function of total dT(pT)<sub>15</sub> concentration according to Scheme 1 using  $K_1 = 2.3 \times 10^7$  M<sup>-1</sup>,  $K_2 = 13$ ,  $K_3 = 1.7 \times 10^8$  M<sup>-1</sup> (Bjornson et al., 1996), and  $K_4 = 3.5 \times 10^5$  M<sup>-1</sup> (Table 2). The relative concentration of each species is given in terms of Rep subunits. The arrows mark the concentrations of dT(pT)<sub>15</sub> chosen for experiments [ $PS$  denotes ( $PS + PS^*$ )].

used the oligodeoxynucleotide dT(pT)<sub>15</sub>, which we have previously shown is short enough so that only one Rep monomer can bind per dT(pT)<sub>15</sub> (Chao & Lohman, 1991; Wong et al., 1992). To facilitate these measurements, it was necessary to determine the Rep and dT(pT)<sub>15</sub> concentrations that favor the exclusive population of each individual species, so that there would be minimal interference from the other species. Bjornson et al. (1996) have recently determined that Scheme 1 represents the minimal kinetic scheme for Rep monomer binding to dT(pT)<sub>15</sub> and subsequent dimerization and have determined the equilibrium constants  $K_1 = 2.3 \times 10^7$  M<sup>-1</sup>,  $K_2 = 13$ , and  $K_3 = 1.7 \times 10^8$  M<sup>-1</sup> under the identical solution conditions used in these studies (BBM at 4 °C). Using these equilibrium constants and Scheme 1, we calculated the equilibrium population distributions of the Rep species ( $P$ ,  $PS$ ,  $P_2S$ ,  $P_2S_2$ ) over a range of Rep and dT(pT)<sub>15</sub> concentrations and these are shown in Figure 2 [note that  $PS$  denotes ( $PS + PS^*$ )]. The distribution of the doubly ligated Rep dimer ( $P_2S_2$ ) is calculated based on the values of  $K_4 \geq 3.5 \times 10^5$  M<sup>-1</sup> and  $K_5 = 1.65 \times 10^5$  M<sup>-1</sup> as determined in this study (as discussed below). Figure 2 shows the species distributions predicted for two concentrations of total Rep monomer [1 nM (Figure 2A) and 0.5  $\mu$ M (Figure 2B)] as a function of [dT(pT)<sub>15</sub>]. The concentrations of dT(pT)<sub>15</sub> used in the ATPase experiments reported here are indicated by the arrows. Figure 2A shows that >97% of total Rep is in the form of  $PS$  at 1 nM Rep and 50 nM dT(pT)<sub>15</sub>, and Figure 2B shows that >99% of all DNA-bound Rep is  $P_2S$  at 0.5  $\mu$ M Rep and 3 nM dT(pT)<sub>15</sub>. Due to the extreme negative cooperativity for DNA binding to the Rep dimer (Wong et al., 1992; Wong & Lohman, 1992; Bjornson et al., 1996), the doubly ligated Rep dimer,  $P_2S_2$ , cannot be formed in isolation at equilibrium, and thus this species was examined by populating it transiently as discussed below.

The predicted distributions of Rep-ss-DNA ligation states shown in Figure 2 were simulated using the equilibrium constants determined for the Rep-dT(pT)<sub>15</sub> interaction in the absence of ATP (Bjornson et al., 1996) and thus reflect the population distributions that exist at the start of each

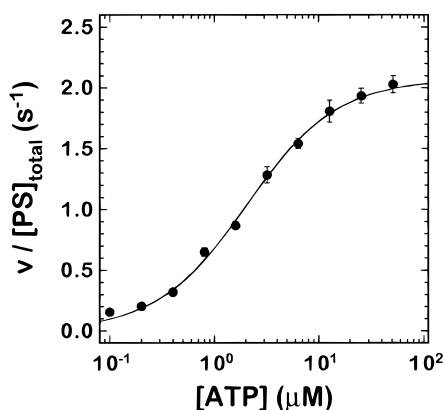


FIGURE 3: ATPase activity of Rep in its PS state. The ATPase activity of ss DNA-ligated Rep monomer (PS) was measured at 1 nM Rep monomers in the presence of 50 nM dT(pT)<sub>15</sub> in BBM buffer with 0.1 mg/mL BSA at 4 °C. At these concentrations, all of the Rep exists in the PS ligation state (see Figure 2A). The solid line represents the best fit of the data to the Michaelis–Menten equation with  $k_{\text{cat}} = 2.17 \pm 0.04 \text{ s}^{-1}$  and  $K_M = 2.05 \pm 0.1 \text{ μM}$ .

experiment, prior to the addition of ATP. These are the correct distributions to consider for the following reasons. The ATPase activities reported in this study were determined from initial velocity measurements within the linear time range. As such, each ATPase activity represents an instantaneous sampling of the initial population of Rep–ss-DNA ligation states before the addition of ATP. If ATP binding and or hydrolysis were to affect the distribution of Rep–DNA ligation states on the time scale of these initial velocity measurements, then the time course of ATP hydrolysis would not be linear since the ATPase activities differ for each ligation state. Furthermore, we have previously shown that the equilibrium constants for dT(pT)<sub>15</sub> binding to form both PS as well as P<sub>2</sub>S are not affected by the binding of the nonhydrolyzable ATP analog AMPPNP (Wong & Lohman, 1992). More recent kinetic evidence from our laboratory has also shown that the ss-DNA ligation states for P<sub>2</sub>S and PS do not change during ATP hydrolysis, although ATP hydrolysis does increase the rate of ss-DNA dissociation from the P<sub>2</sub>S<sub>2</sub> state (K. P. Bjornson et al., manuscript in preparation). Accordingly, the time course of ATP hydrolysis by P<sub>2</sub>S<sub>2</sub> is nonlinear, reflecting a change in the population distribution of Rep–ss-DNA ligation states. However, even the time course of ATP hydrolysis by P<sub>2</sub>S<sub>2</sub> is linear within the first 10 s, and thus these initial velocities reflect an accurate sampling of even the P<sub>2</sub>S<sub>2</sub> ligation state (see Results and Discussion).

**ATPase Activity of Rep Monomer Bound to dT(pT)<sub>15</sub> (PS).** The ATPase activity of Rep monomer bound to ss DNA (PS) was determined in the presence of excess dT(pT)<sub>15</sub> (50 nM) at 1 nM Rep at 4 °C in BBM buffer containing BSA (0.1 mg/mL). Based on the simulations shown in Figure 2A, >97% of the Rep is monomeric and bound to DNA under these conditions; the remaining protein is present as unligated Rep monomers (3%) and P<sub>2</sub>S (<1%). The steady-state rates of ATP hydrolysis as a function of ATP concentration are shown in Figure 3 and are well described by a rectangular hyperbola with  $k_{\text{cat}} = 2.10 \pm 0.04 \text{ s}^{-1}$  and  $K_M = 2.30 \pm 0.07 \text{ μM}$ . Inclusion of BSA was necessary in order to stabilize the Rep protein at such low concentrations. BSA did not influence the ATPase activity of Rep in experiments performed at higher Rep concentrations (data not shown).

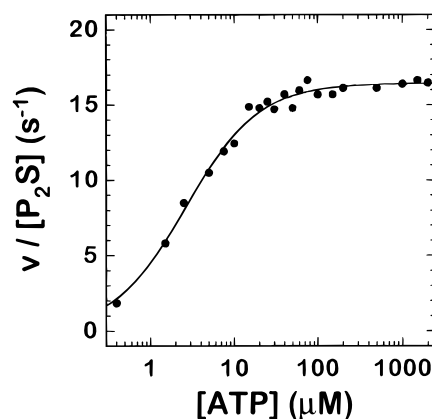


FIGURE 4: ATPase activity of Rep in its P<sub>2</sub>S state. The ATPase activity of P<sub>2</sub>S was measured at 5 μM Rep monomers in the presence of 3 nM dT(pT)<sub>15</sub> in BBM buffer at 4 °C. Under these conditions, all of the DNA is bound to Rep in its P<sub>2</sub>S state (see Figure 2B). The large excess of unligated Rep monomers have negligible ATPase activity and do not interfere with the assay. The solid line represents the best fit of the data to the Michaelis–Menten equation with  $k_{\text{cat}} = 16.5 \pm 0.2 \text{ s}^{-1}$  and  $K_M = 2.7 \pm 0.2 \text{ μM}$ .

**ATPase Activity of the Half-Ligated Rep Dimer (P<sub>2</sub>S).** The ATPase activity of the half-ligated Rep dimer, P<sub>2</sub>S, was determined under conditions of excess Rep (0.5 μM) and limiting dT(pT)<sub>15</sub> (30 nM). The simulations in Figure 2B show that >99% of all Rep bound to DNA is dimeric and in the P<sub>2</sub>S ligation state under these conditions. The majority of the Rep protein is present as the unligated monomer, P. However, since the ATPase activity of the unligated Rep monomer [ $0.0021 \text{ s}^{-1}$  (Moore & Lohman, 1994b)] is negligible compared to the Rep dimers, this population is not detectable in a steady-state ATPase measurement. Furthermore, the ATP concentrations were always in sufficient excess over the total Rep monomer concentration to ensure that binding of ATP by Rep monomers did not compete with binding of ATP by P<sub>2</sub>S. Initial velocities normalized with respect to the concentration of P<sub>2</sub>S, which equals the total [dT(pT)<sub>15</sub>], are plotted as a function of ATP concentration in Figure 4. The data are well described by a rectangular hyperbola with  $k_{\text{cat}} = 16.5 \pm 0.2 \text{ s}^{-1}$  and  $K_M = 2.7 \pm 0.2 \text{ μM}$ .<sup>2</sup>

**ATPase Activity of the Fully Ligated Rep Dimer (P<sub>2</sub>S<sub>2</sub>).** We first attempted to measure the ATPase activity of P<sub>2</sub>S<sub>2</sub> by forming P<sub>2</sub>S<sub>2</sub> at high dT(pT)<sub>15</sub> concentration. Toward this end, we titrated 2 μM Rep monomers with dT(pT)<sub>15</sub> and measured the ATPase activity as a function of [dT(pT)<sub>15</sub>]. The results of one such experiment are shown in Figure 5. The observed ATPase activity, however, was not a simple function of [dT(pT)<sub>15</sub>] but was multiphasic with an initial increase up to 1 μM dT(pT)<sub>15</sub>, corresponding to a ratio of 2 Rep monomers per dT(pT)<sub>15</sub>, but then decreased sharply followed by a more gradual increase upon further addition of dT(pT)<sub>15</sub>. This behavior can be qualitatively explained using the model of Bjornson et al. (1996) shown in Scheme 1. However, we were unable to obtain a quantitative value for the  $k_{\text{cat}}$  of the ATPase of P<sub>2</sub>S<sub>2</sub> because this is strongly coupled to the equilibrium constants,  $K_4$  or  $K_5$ , used to generate the fit, i.e., any value of  $k_{\text{cat}}$  could be accommodated by a compensating change in  $K_4$  or  $K_5$ . The solid line in

<sup>2</sup> Recent determinations of the  $k_{\text{cat}}$  for P<sub>2</sub>S under the same solution conditions yield a value of  $18 \pm 0.5 \text{ s}^{-1}$ , and we have used this value in our global fitting to determine the value of  $k_{\text{cat}}$  for P<sub>2</sub>S<sub>2</sub>.

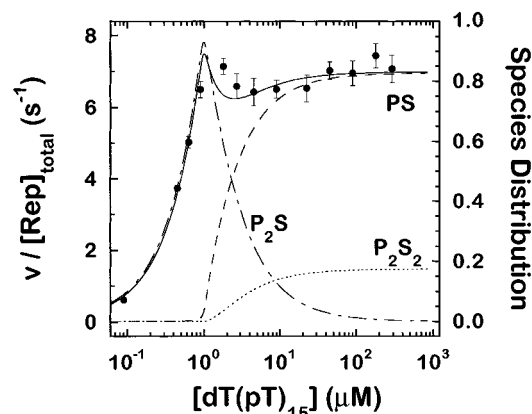


FIGURE 5: Dependence of Rep ATPase activity on  $dT(pT)_{15}$  concentration. The ATPase activity of Rep was measured at  $2 \mu M$  Rep monomers as a function of  $dT(pT)_{15}$  concentration. The observed rates were normalized with respect to total Rep monomer concentration. These rates showed a complex dependence on  $dT(pT)_{15}$  concentration, reflecting changes in Rep- $dT(pT)_{15}$  ligation states. The distributions of the different Rep-DNA species at each  $dT(pT)_{15}$  concentration were simulated using the model in Scheme 1 and the equilibrium constants:  $K_1 = 2.3 \times 10^7 M^{-1}$ ,  $K_2 = 13$ , and  $K_3 = 1.7 \times 10^8 M^{-1}$  (Bjornson et al., 1996). A value for  $K_4 = 2.5 \times 10^5 M^{-1}$  was used to obtain the best fit of the data. The solid line represents the ATPase activity calculated from this simulated distribution of states using  $k_{cat}$  values of  $2 s^{-1}$  for PS,  $16.5 s^{-1}$  for  $P_2S$ , and  $71 s^{-1}$  for  $P_2S_2$ .

Table 1: ATPase Activities of Rep Species<sup>a</sup>

	$k_{cat} (s^{-1})$	$K_M (\mu M)$
P	$2 \times 10^{-3}^b$	$7 \times 10^{-3}^b$
PS	$2.17 \pm 0.04^c$	$2.05 \pm 0.1^c$
$P_2S$	$16.5 \pm 0.2$	$2.7 \pm 0.2$
$P_2S_2$	$71 \pm 2.5$	

<sup>a</sup> Assayed in BBM buffer at  $4^\circ C$ . <sup>b</sup> From Moore and Lohman (1994a). <sup>c</sup> Assayed in BBM buffer plus  $0.1 mg/mL$  BSA at  $4^\circ C$ .

Figure 5 is the predicted ATPase activity based on simulations using Scheme 1, the equilibrium constants  $K_1$ ,  $K_2$ , and  $K_3$  (Bjornson et al., 1996), the  $k_{cat}$  values for PS and  $P_2S$  (Table 1), and  $K_4$  and  $K_5$  and  $k_{cat} = 71 s^{-1}$  for  $P_2S_2$  as determined below. The species distribution calculated from Scheme 1 is also shown in Figure 5.

Under the conditions of the experiment described in Figure 5, we were unable to populate  $P_2S_2$  sufficiently at equilibrium due to the high degree of negative cooperativity for DNA binding to the Rep dimer (Wong et al., 1992; Wong & Lohman, 1992). This can be seen from the calculated species distribution in Figure 5. In fact, under these solution conditions at high  $[dT(pT)_{15}]$ , the observed ATPase activity has contributions from a large population of PS with a modest ATPase activity and a small population of  $P_2S_2$  with a large ATPase activity.

In order to obtain an accurate measurement of the ATPase activity of  $P_2S_2$ , it was necessary to achieve a higher population of  $P_2S_2$ . However, because  $P_2S_2$  is not favored at equilibrium, it had to be populated transiently. We accomplished this by pre-forming a solution of  $P_2S$ , which was then mixed with excess  $dT(pT)_{15}$  in order to transiently populate  $P_2S_2$ , while monitoring the ATPase activity as a function of time as the system reequilibrates. Since the binding of  $dT(pT)_{15}$  by  $P_2S$  is bimolecular, at sufficiently high  $dT(pT)_{15}$  concentrations, the rate of formation of  $P_2S_2$  exceeds the rate of dissociation of the  $P_2S_2$  dimer resulting

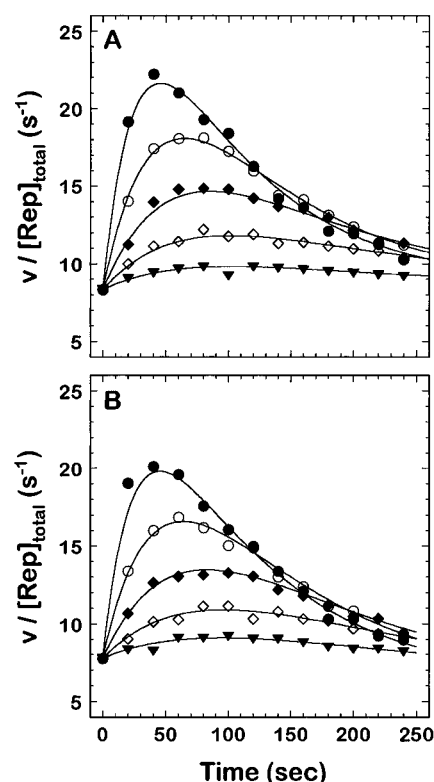


FIGURE 6: Kinetics of the transient formation of  $P_2S_2$ .  $P_2S_2$  was transiently populated by the addition of excess  $dT(pT)_{15}$  to pre-formed  $P_2S$ . Initial rapid DNA binding leads to a transient increase in ATPase activity corresponding to transient formation of  $P_2S_2$  followed by a slower decrease in ATPase activity corresponding to the disproportionation of  $P_2S_2$  to  $2PS$ . Conditions were performed in BBM buffer at  $4^\circ C$  starting with (A)  $1.0 \mu M$  Rep monomers and  $0.6 \mu M$   $dT(pT)_{15}$ , or (B)  $0.5 \mu M$  Rep monomers and  $0.3 \mu M$   $dT(pT)_{15}$ . At  $t = 0$ ,  $dT(pT)_{15}$  was added to a final concentration of  $100 (\bullet)$ ,  $50 (\circ)$ ,  $25 (\blacklozenge)$ ,  $12.5 (\diamond)$ , or  $6.25 \mu M (\blacktriangledown)$ . Solid lines represent kinetic simulations of the data using Scheme 1 and the best fit parameters obtained from global analysis of all data sets in both panels using FITSIM and KINSIM. Best-fit parameters for  $k_{cat}$  of  $P_2S_2$  was  $71 \pm 2.5 s^{-1}$ . The apparent second-order rate constant for DNA binding to  $P_2S$ ,  $k_4 = 387 \pm 3 M^{-1} s^{-1}$ . The rate of disproportionation of  $P_2S_2$  to  $2PS$ ,  $k_5 = 0.0079 \pm 0.0001 s^{-1}$ .

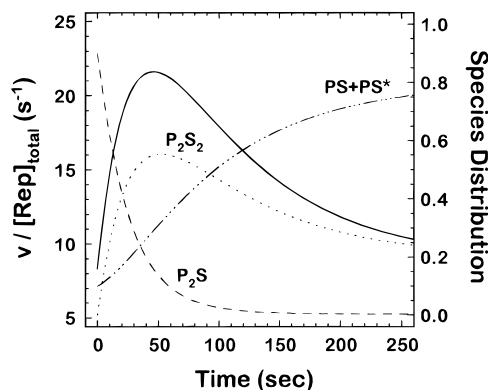
in the transient accumulation of  $P_2S_2$ . The change in ATPase activity during this transient can be used to determine the ATPase activity of  $P_2S_2$ .

The results from such a series of experiments are shown in Figure 6A where we preincubated  $1 \mu M$  Rep monomers with  $0.6 \mu M$   $dT(pT)_{15}$  to form  $P_2S$ , followed by the addition of  $6.25$ ,  $12.5$ ,  $25.5$ ,  $50$ , or  $100 \mu M$   $dT(pT)_{15}$  at  $t = 0$ . At  $20 s$  intervals, aliquots were removed and assayed for ATPase activity to obtain initial velocities,  $v$ . In all cases, immediately after the addition of excess  $dT(pT)_{15}$ , the ATPase activity increased transiently and then decreased to its new equilibrium value. The rate of the transient increase in ATPase activity and its amplitude were dependent on the concentration of  $dT(pT)_{15}$  added, while the rate of decay of the transient was not. This behavior is consistent with transient formation of  $P_2S_2$  followed by dissociation of the dimer to yield a mixture of  $PS^*$ ,  $PS$  and  $P_2S_2$  at equilibrium. Similar results were also obtained in experiments performed with starting concentrations of  $0.5 \mu M$  Rep and  $0.3 \mu M$   $dT(pT)_{15}$  as shown in Figure 6B.

In order to determine the kinetic rate constants in Scheme 1 and a value of  $k_{cat}$  for  $P_2S_2$  from these experiments, both sets of data in Figure 6 were analyzed simultaneously using

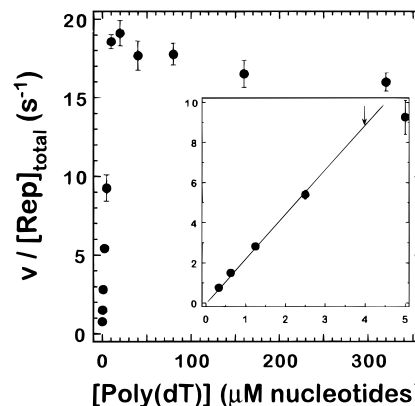
Table 2: Kinetic and Thermodynamic Parameters for Formation of  $P_2S_2$ <sup>a</sup>

$n$	$k_n$ ( $M^{-1} s^{-1}$ )	$k_{-n}$ ( $s^{-1}$ )	$K$ ( $\mu M^{-1}$ )
4	$3.87 \pm 0.03 \times 10^2$	$< 1.1 \times 10^{-3}$	$> 3.5 \times 10^5$
5	$1.3 \pm 0.2 \times 10^3$	$7.9 \pm 0.1 \times 10^{-3}$	$1.65 \times 10^5$

<sup>a</sup> Assayed in BBM buffer at 4 °C.FIGURE 7: Kinetics of formation of the different Rep-dT(pT)<sub>15</sub> species during the transient formation of  $P_2S_2$ . The time course of formation of the different Rep-dT(pT)<sub>15</sub> species for the experiment in Figure 6A at 1  $\mu M$  Rep and 100  $\mu M$  dT(pT)<sub>15</sub> was simulated using KINSIM and the best-fit parameters determined from the experiments in Figure 6. The solid line represents the simulated ATPase activity. The fractions of Rep monomers present as  $P_2S$ ,  $P_2S_2$ , and  $PS$  are indicated.

the numerical nonlinear fitting program FITSIM (Zimmerle & Frieden, 1989). The dependence on dT(pT)<sub>15</sub> concentration of the rate of increase of the transient provides information on  $k_4$ , the association rate constant for binding dT(pT)<sub>15</sub> to  $P_2S$ . The amplitude of this transient is determined by the net increase in  $k_{cat}$  for the ATPase on forming  $P_2S_2$  from  $P_2S$ . Furthermore, the rate of decay of the transient gives the rate of dissociation of  $P_2S_2$  to form  $2PS^*$ . From this analysis, we were able to obtain the best fit values for  $k_4 = 387 \pm 3 M^{-1} s^{-1}$ ,  $k_5 = 1.3 \pm 0.2 \times 10^3 M^{-1} s^{-1}$ ,  $k_{-5} = 7.9 \pm 0.1 \times 10^{-3} s^{-1}$  (Table 2), and  $k_{cat} = 71 \pm 2.5 s^{-1}$ . The rate of dissociation of DNA from  $P_2S_2$ ,  $k_{-4}$ , could only be determined as an upper limit of  $1.1 \times 10^{-3}$ . The value of the rate constant,  $k_{-3}$ , for dissociation of  $P_2S$  to  $PS^*$  and  $P$  was fixed at  $0.0025 s^{-1}$  as determined by Bjornson et al. (1996). The ATPase activity of  $P_2S$  was constrained to  $18 s^{-1}$ . The remaining kinetic parameters were constrained to the values determined by Bjornson et al. (1996) ( $k_1 = 3.3 \times 10^7 M^{-1} s^{-1}$ ,  $k_{-1} = 1.4 s^{-1}$ ,  $k_2 = 2.7 s^{-1}$ ,  $k_{-2} = 0.21 s^{-1}$ ,  $k_3 = 4.5 \times 10^5 M^{-1} s^{-1}$ ,  $k_{-3} = 2.7 \times 10^{-3} M^{-1} s^{-1}$ ). As can be seen from the simulations in Figure 6, these rate constants and the values of  $k_{cat}$  for ( $PS + PS^*$ ),  $P_2S$ , and  $P_2S_2$  provide an excellent description of all of the experiments. Figure 7 shows the time dependence of the Rep species distribution for the experiment in Figure 6A performed at 100  $\mu M$  dT(pT)<sub>15</sub>.

**ATPase Activity of Rep Bound to Poly(dT).** We also measured the ATPase activity of Rep when bound to poly(dT) in order to compare with the ATPase activities of the different Rep-dT(pT)<sub>15</sub> species. A series of ATPase measurements were performed at a total Rep concentration of 0.5  $\mu M$  monomers and poly(dT) (nucleotide) concentrations of 320, 160, 80, 40, 20, 10, 5, 2.5, 1.25, 0.625, and 0.32  $\mu M$  in BBM buffer and 2 mM ATP at 4 °C. The steady-state rates of ATP hydrolysis were normalized with respect to total

FIGURE 8: ATPase activity of Rep bound to poly(dT). The ATPase activity of Rep (0.5  $\mu M$  Rep monomers) was measured as a function of poly(dT) concentration in BBM buffer at 4 °C. The observed ATPase activity was linearly dependent on DNA concentration up to 2.5  $\mu M$  (total nucleotides) poly(dT) (see inset). Linear extrapolation of this line to an observed rate of 9  $s^{-1}$  per monomer, corresponding to the maximum  $P_2S$  rate of 18  $s^{-1}$  per dimer, yielded a [poly(dT)] of 4  $\mu M$  (corresponding to 16 nucleotides per  $P_2S$ ). The ATPase activity increased further to 19  $s^{-1}$  per monomer at a nucleotide concentration of 10–20  $\mu M$  but decreased on further addition of poly(dT).

Rep monomer concentration and plotted as a function total poly(dT) nucleotide concentration in Figure 8. The specific ATPase activity increases with increasing nucleotide concentration to a maximum measured rate of 19  $s^{-1}$  at 10.0  $\mu M$  but then decreases to 16  $s^{-1}$  at the highest poly(dT) concentration examined (320  $\mu M$ ).

## DISCUSSION

A general feature of all DNA helicases is that nucleoside triphosphatase activity is stimulated by DNA binding (Matson, 1991; Matson & Kaiser-Rogers, 1990). In fact, Moore and Lohman (1994a,b) have shown unambiguously that Rep protein monomers can bind and hydrolyze ATP even in the absence of DNA, but that ss-DNA binding to the Rep monomer greatly stimulates this activity. We have also previously demonstrated qualitatively that Rep dimerization further stimulates its ATPase activity (Wong et al., 1993). In this report, we have directly determined the steady-state ATPase activities of all three distinct ss-DNA ligation states of Rep,  $PS$ ,  $P_2S$ , and  $P_2S_2$  (Table 1). Our results indicate that the ATPase activity of Rep is greatly influenced by both its oligomeric state and its ss-DNA ligation state, with each Rep species possessing dramatically different ATPase activity. Thus the intrinsic basal ATPase activity of unligated Rep monomer,  $P$ , is stimulated by a  $10^3$ -fold from  $2.1 \times 10^{-3} s^{-1}$  (Moore & Lohman, 1994b) to  $2.17 s^{-1}$  on binding dT(pT)<sub>15</sub> to form the ss-DNA bound monomer,  $PS$ . The ATPase activity is further enhanced by a factor of 8–9 on Rep dimerization to form the half-ligated dimer state,  $P_2S$ , with an ATPase activity of  $16.5 s^{-1}$ . Further binding of dT(pT)<sub>15</sub> to the second site of the Rep dimer to form  $P_2S_2$  results in an additional 4.5-fold increase in activity to  $71 s^{-1}$ . These results show clearly the high degree of allosteric linkage that exists between DNA binding sites and the ATPase active sites on both subunits of the Rep dimer. These results also call into question the utility of macroscopic steady-state ATPase measurements in addressing mechanistic questions at a molecular level in the absence of information about the thermodynamic and kinetic parameters that govern the

species distribution of ligation states for the reaction conditions under study. These and other implications of our results are discussed below.

**Effects of ss-DNA Binding and Protein Dimerization on Rep ATPase Activity.** The largest influence on Rep ATPase activity occurs upon binding ss DNA to the Rep monomer to form the PS species. This results in a 1000-fold increase in  $k_{\text{cat}}$  and a 300-fold increase in  $K_M$  relative to the unligated monomer, P. The mechanism of binding and hydrolysis of ATP by P is well understood (Moore & Lohman, 1994a,b). ATP binding occurs by a two-step mechanism involving initial binding followed by a conformation change. ATP hydrolysis is rate-limiting at  $2 \times 10^{-3} \text{ s}^{-1}$ . The large overall equilibrium constant for ATP binding to Rep monomer under the conditions used here ( $K = 1.4 \times 10^8 \text{ M}^{-1}$ ;  $K_d = 7 \text{ nM}$ ) reflects the additional favorable free energy gained in the conformation change step. Since ATP hydrolysis is rate-limiting under these conditions, the  $K_M$  for ATP hydrolysis by Rep monomer, P, should also equal 7 nM. The increase of both  $k_{\text{cat}}$  and  $K_M$  on binding ss-DNA (dT(pT)<sub>15</sub>) to form PS likely reflects a change in rate-limiting step from chemistry to the conformation change prior to chemistry. However, more direct measurements of the kinetics of nucleotide binding by PS are required to test this hypothesis.

We have also previously shown that the specific activity of Rep in the presence of excess dT(pT)<sub>15</sub> undergoes a Rep concentration-dependent increase in the range from 10 to 100 nM total Rep monomer (Wong et al., 1993), suggesting that Rep dimerization stimulates the ATPase activity. However, the observed transition was too steep to be accounted for by just dimerization alone and thus likely reflects both dimerization and changes in ss-DNA ligation states. Consequently, we were unable to quantitatively resolve the effects of dimerization on ATPase activity from the effects of DNA binding in that study. In this report, we were able to use the kinetic and thermodynamic parameters for dT(pT)<sub>15</sub> binding and protein dimerization determined by Bjornson et al. (1996) to optimize reaction conditions such that we were able to populate exclusively the P<sub>2</sub>S state. The measured macroscopic ATPase activity for this species is  $16.5 \text{ s}^{-1}$  per dimer with an apparent  $K_M$  for ATP of  $2.7 \mu\text{M}$  assuming only one active site per dimer. This result shows a clear 8-fold increase in activity upon forming P<sub>2</sub>S from PS.

The ATP concentration dependence of the steady-state ATPase activity of P<sub>2</sub>S is well described by a rectangular hyperbola with no evidence for the binding and hydrolysis of more than one ATP per P<sub>2</sub>S dimer. However, isolated Rep monomers, P, possess a single nucleotide binding site (Moore & Lohman, 1994a,b), and the studies reported here indicate that Rep monomers bound to ss-DNA, PS, also bind ATP. Therefore, Rep dimers must possess two ATP binding sites. Furthermore, we have additional evidence from studies of Rep mutants (I. Wong, unpublished experiments) as well as from DNA dissociation kinetics (K. Bjornson, unpublished experiments) that both subunits of the P<sub>2</sub>S Rep dimer are capable of binding and hydrolyzing ATP. However, as with all systems with multiple ligand binding sites, it is often difficult to resolve the different ATP sites based on steady-state experiments, and for the P<sub>2</sub>S dimer it appears fortuitous that the steady-state rates of ATP hydrolysis can be described by a one ATP site model. In fact, these results emphasize

that the observation that a limited set of steady-state ATPase measurements can be described by Michaelis–Menten kinetics does not represent sufficient evidence to conclude that a helicase possesses only a single ATP binding site, especially when the protein undergoes self-assembly.

**Allosteric Control of ATPase Activity at Both ATP Sites of the Rep Dimer by ss-DNA Binding in P<sub>2</sub>S<sub>2</sub>.** The doubly ligated Rep dimer state, P<sub>2</sub>S<sub>2</sub>, is difficult to populate at equilibrium due to the negative cooperativity for binding ss-DNA in the second site (Wong et al., 1992; Wong & Lohman, 1992; Bjornson et al., 1996). However, we were able to form transiently a sufficiently high population of P<sub>2</sub>S<sub>2</sub> to measure its ATPase activity. The best fit of our data at two protein concentrations and five DNA concentrations allowed us to determine the specific ATPase activity for P<sub>2</sub>S<sub>2</sub> of  $71 \pm 2.5 \text{ s}^{-1}$ . This represents a 4.5-fold increase in activity relative to P<sub>2</sub>S on binding ss-DNA to the second subunit of the Rep dimer. If the ATPase activities of the two Rep subunits are independently stimulated by binding of ss-DNA to each individual subunit, then one would expect the ATPase activity of P<sub>2</sub>S to result from stimulation of only one subunit, and, therefore, P<sub>2</sub>S<sub>2</sub> would be expected to have twice the activity as P<sub>2</sub>S. Our results show clearly that the ATPase activity of P<sub>2</sub>S<sub>2</sub> well exceeds twice that of P<sub>2</sub>S and therefore provide direct evidence that the binding of ss DNA exerts global influences on the ATPase activities of both subunits.

As with P<sub>2</sub>S, one must be careful not to overinterpret these results due to the macroscopic nature of these measurements. Although we know that the allosteric effects of DNA binding on ATPase activity clearly extends across the dimer interface, we cannot determine based solely on these results alone whether both potential ATPase sites of the P<sub>2</sub>S<sub>2</sub> dimer are active. Since we have independent evidence that both ATP sites on P<sub>2</sub>S are active at least in binding ATP (see discussion above), we feel it is likely that the same would hold true for P<sub>2</sub>S<sub>2</sub>.

**Kinetics of DNA Induced Dissociation of P<sub>2</sub>S<sub>2</sub>.** In the process of analyzing the kinetics experiments in which P<sub>2</sub>S<sub>2</sub> was formed transiently to obtain  $k_{\text{cat}}$  for the ATPase of P<sub>2</sub>S<sub>2</sub>, we found that we were able also to resolve the kinetic rate constant for dissociation of P<sub>2</sub>S<sub>2</sub> to 2PS, a parameter which was not previously available to us. In previous fluorescence stopped-flow studies of the kinetic mechanism of Rep monomer DNA binding and DNA-induced Rep dimerization, Bjornson et al. (1996) showed unambiguously that binding dT(pT)<sub>15</sub> to P<sub>2</sub>S increases the rate of release of the ss-DNA that was originally bound to P<sub>2</sub>S. In that experiment, P<sub>2</sub>S was pre-formed using a fluorescent oligodeoxynucleotide and then mixed with an excess of a nonfluorescent ss-DNA chase, dT(pT)<sub>15</sub>, while monitoring the net rate of dissociation of the fluorescent oligonucleotide. The net rate of dissociation of the fluorescent ss-DNA varied hyperbolically as a function of the concentration of the chase reaching an asymptotic limit at infinite dT(pT)<sub>15</sub> concentration of  $6.7 \times 10^{-3} \text{ s}^{-1}$ . This rate constant equals the sum of the rate constants for all possible kinetic pathways for the loss of DNA from P<sub>2</sub>S<sub>2</sub>. In this instance, there are two such pathways: (1) direct dissociation of ss-DNA from P<sub>2</sub>S<sub>2</sub> to form P<sub>2</sub>S plus S, and (2) dissociation of the P<sub>2</sub>S<sub>2</sub> dimer to form 2 PS, followed by rapid dissociation of ss DNA from the PS monomers. However, these two pathways could not be distinguished based on those experiments (Bjornson et al., 1996).

The transient kinetic studies reported here monitoring formation and decay of  $P_2S_2$  by its ATPase activity allow us to determine directly the kinetic constants for its formation from  $P_2S$  as well as for its dissociation to 2 PS. The global best-fit values for these parameters agree well with those measured independently by Bjornson et al. (1996) using fluorescence stopped-flow methods. Furthermore, because of the biphasic nature of the time courses, there must be at least two different kinetic steps: one responsible for each phase. Since the rise of the transient is clearly dependent on the  $dT(pT)_{15}$  concentration, it must be assigned to the binding of  $dT(pT)_{15}$  to  $P_2S$  to form  $P_2S_2$ . Consequently, the decay phase of the transient cannot be assigned to the dissociation of the DNA as that would violate microscopic reversibility. Therefore, we can unambiguously assign this phase to the dissociation of  $P_2S_2$  to form 2 PS. The global analysis of the data yields a rate of  $0.0079 \pm 0.0001$  for this phase (Table 2). Since this value quantitatively accounts for the value of  $0.0067 \text{ s}^{-1}$  measured by Bjornson et al. (1995), we conclude that dimer dissociation, rather than DNA dissociation, is the predominant pathway for the exchange of ss-DNA observed in the absence of nucleotide (Bjornson et al., 1996).

*Effects of ss-DNA Length and Concentration on Rep ATPase Activity.* The negative cooperativity that causes the doubly-ligated Rep dimer,  $P_2S_2$ , to dissociate to 2 PS is also apparent in the results of the  $dT(pT)_{15}$  and poly(dT) experiments. In both experiments, the observed ATPase activity as a function of DNA concentration is multiphasic. In both cases, the observed ATPase activity initially increases with DNA concentration. However, in the concentration range after  $P_2S$  becomes fully saturated, a decrease in ATPase activity is observed on further addition of DNA. In the case of  $dT(pT)_{15}$ , this intermediate phase is then followed by another slight increase (see Figure 5). As the specific activity of  $P_2S_2$  is 4.5-fold higher than that of  $P_2S$ , this intermediate phase where the observed activity drops cannot be accounted for by the formation of  $P_2S_2$  from  $P_2S$ . Instead, as the species distribution plot in Figure 5 clearly shows, this intermediate loss of activity arises from the formation of PS as a result of dissociation of  $P_2S_2$  following the binding of  $dT(pT)_{15}$  to the second site of  $P_2S$ . Furthermore, the final plateau reached at high  $dT(pT)_{15}$  concentrations reflects primarily the activity of a large fraction of PS with a modest contribution from a small fraction of  $P_2S_2$ .

We were able to analyze the  $dT(pT)_{15}$  data in this fashion only because we know all the relevant equilibrium constants for Scheme 1 as well as the specific activity of each ligation state. The interpretation of the poly(dT) experiments, however, is more complex. To a first approximation we can extrapolate from our knowledge of the Rep- $dT(pT)_{15}$  system; however, we note two significant differences between the  $dT(pT)_{15}$  data and the poly(dT) data. First, the maximum observed ATPase activity in the poly(dT) experiment exceeds that observed in the  $dT(pT)_{15}$  experiment. Whereas the maximum observed rate with  $dT(pT)_{15}$  is contributed solely by  $P_2S$ , it is clear that the maximum observed rate with poly(dT) is at least 2-fold higher than the specific activity of  $P_2S$  and must therefore reflect some contribution from  $P_2S_2$ . Secondly, unlike the  $dT(pT)_{15}$  data, the poly(dT) data show a much more gradual loss of ATPase activity at higher DNA concentrations. These two observations suggest that the  $P_2S_2$ /PS equilibrium is affected by the local concentrations of

DNA bound Rep monomers on the poly(dT). Thus, more  $P_2S_2$  is formed at low [poly(dT)] (high binding density on poly(dT)); however, the addition of more poly(dT) lowers the average binding density of Rep on poly(dT) resulting in a net dissociation of Rep dimers to form PS.

*Can One Use Macroscopic ATPase Measurements To Infer Mechanistic Information?* In numerous studies of helicases, mechanistic conclusions have often been drawn based solely on steady-state ATPase measurements. Examples range from estimates of the number of ATP molecules hydrolyzed per base pair unwound (Yarranton & Gefter, 1979; Kornberg et al., 1978; Arai & Kornberg, 1981; Roman & Kowalczykowski, 1989; Korangy & Julin, 1994) to conclusions about ATP-driven unidirectional translocation (Liu & Alberts, 1981; Matson et al., 1983; Matson & George, 1987; Lahue & Matson, 1988; Young et al., 1994a,b; Raney & Benkovic, 1995) to studies of mutants with "uncoupled" ATP and unwinding activities (George et al., 1994). Despite the known oligomeric nature of all the helicases involved in these studies, the possibility of multiple ATP sites has generally not been considered. Similarly, the effects of the distribution of DNA-ligation states and changes in that distribution as a result of changes in experimental parameters are generally not considered. Yet, mechanistic conclusions have been drawn based on changes in ATPase activities that are often as small as factors of 3 or 4 (Young et al., 1994a,b; Raney & Benkovic, 1995). Our results with Rep and  $dT(pT)_{15}$  suggest that these modest differences can be due to changes in the distribution of DNA ligation states, and thus such effects must be explicitly considered in the interpretation of such experiments.

*Summary.* We have measured the steady-state ATPase activities of each distinct ss-DNA ligation state of Rep monomer and dimer using  $dT(pT)_{15}$ . Our results indicate that the ATPase activity of the Rep protein is dramatically influenced by both its oligomerization and its ss-DNA ligation state. Furthermore, we have shown that the binding of ss-DNA allosterically regulates the ATPase activity of the dimeric Rep helicase. Previously we have shown that nucleotide (ADP and AMPPNP) binding allosterically regulates DNA binding and that the distribution of ss DNA ligation states can be dramatically affected by the binding of nucleotides (Wong & Lohman, 1992). Our observation that the fully ligated dimer,  $P_2S_2$ , has 4.5 times the activity of the half-ligated dimer,  $P_2S$ , shows unequivocally that the binding of ss-DNA to the second subunit has global effects that are transmitted across the dimer interface. These allosteric effects and the dramatic differences between ss-DNA ligation states of Rep reported here likely play a functionally significant role in the energy transduction cycle. Pre-steady-state kinetic experiments are currently underway to address the mechanistic questions concerning the roles of the two nucleotide binding sites and how ATP binding and hydrolysis at these two sites are coupled to each other and to DNA binding and release.

As the observed ATPase activity under any particular reaction condition reflects only the macroscopic population average of the activities of all the ligation states present, the large differences between the activities of the various ligation states means that it is quite easy to obtain significant changes in observed ATPase activities as a result of relatively small changes in the distribution of ligation states. Therefore, care should be exercised in drawing mechanistic conclusions



based solely on observed differences in steady-state ATPase activities. This holds also for hexameric helicases, since the potential number of oligomerization and DNA ligation states with different ATPase activities is increased well beyond those that must be considered for a dimer such as the Rep helicase.

## ACKNOWLEDGMENT

We thank Bill van Zante for purification of the oligodeoxynucleotides and Janid Ali for his comments on the manuscript.

## REFERENCES

- Amaratunga, M., & Lohman, T. M. (1993) *Biochemistry* 32, 6815–6820.
- Arai, N., & Kornberg, A. (1981) *J. Biol. Chem.* 256, 5294–5298.
- Arai, N., Arai, K. I., & Kornberg, A. (1981) *J. Biol. Chem.* 256, 5287–5293.
- Barshop, B. A., Wrenn, R. F., & Frieden, C. (1983) *Anal. Biochem.* 130, 134–145.
- Bjornson, K. P., Amaratunga, M., Moore, K. J. M., & Lohman, T. M. (1994) *Biochemistry* 33, 14306–14316.
- Bjornson, K. P., Moore, K. J. M., & Lohman, T. M. (1996) *Biochemistry* 35, 2268–2282.
- Bridges, B. A., & von Wright, A. (1981) *Mutat. Res.* 82, 229–238.
- Brown, W. C., & Romano, L. J. (1989) *J. Biol. Chem.* 264, 6748–6754.
- Calendar, R., Lindqvist, B., Sironi, G., & Clark, A. J. (1970) *Virology* 40, 72–83.
- Chao, K., & Lohman, T. M. (1991) *J. Mol. Biol.* 221, 1165–1181.
- Colasanti, J., & Denhardt, D. T. (1987) *Mol. Gen. Genet.* 209, 382–390.
- George, J. W., Brosh Jr., R. M., & Matson, S. W. (1994) *J. Mol. Biol.* 235, 424–435.
- Hanawalt, P. C. (1994) *Science* 266, 1957–1958.
- Korangy, F., & Julin, D. A. (1994) *Biochemistry* 33, 9552–9560.
- Kornberg, A., Scott, J. F., & Bertsch, L. L. (1978) *J. Biol. Chem.* 253, 3298–3304.
- Lahue, E. E., & Matson, S. W. (1988) *J. Biol. Chem.* 263, 3208–3215.
- Lane, H. E. D., & Denhardt, D. T. (1974) *J. Bacteriol.* 120, 805–814.
- Lane, H. E. D., & Denhardt, D. T. (1975a) *J. Bacteriol.* 120, 805–814.
- Lane, H. E. D., & Denhardt, D. T. (1975b) *J. Mol. Biol.* 97, 99–112.
- Liu, C. C., & Alberts, B. (1981) *J. Biol. Chem.* 256, 2813–2820.
- Lohman, T. M. (1992) *Mol. Microbiol.* 6, 5–14.
- Lohman, T. M. (1993) *J. Biol. Chem.* 268, 2269–2272.
- Lohman, T. M., & Bujalowski, W. (1988) *Biochemistry* 27, 2260–2265.
- Lohman, T. M., & Bjornson, K. P. (1996) *Annu. Rev. Biochem.* 65, 169–214.
- Lohman, T. M., Chao, K., Green, J. M., Sage, S., & Runyon, G. (1989) *J. Biol. Chem.* 264, 10139–10147.
- Matson, S. W. (1991) *Prog. Nucleic Acid Res.* 40, 289–326.
- Matson, S. W., & George, J. W. (1987) *J. Biol. Chem.* 262, 2066–2076.
- Matson, S. W., & Kaiser-Rogers, K. A. (1990) *Annu. Rev. Biochem.* 59, 289–329.
- Matson, S. W., Tabor, S., & Richardson, C. C. (1983) *J. Biol. Chem.* 258, 14017–14024.
- Matson, S. W., Bean, D. W., & George, J. W. (1994) *Bioessays* 16, 13–22.
- Moore, K. J. M., & Lohman, T. M. (1994a) *Biochemistry* 33, 14565–14578.
- Moore, K. J. M., & Lohman, T. M. (1994b) *Biochemistry* 33, 14550–14564.
- Moore, K. J. M., & Lohman, T. M. (1995) *Biophys. J.* 68, 180s–185s.
- Raney, K. D., & Benkovic, S. J. (1995) *J. Biol. Chem.* 270, 22236–22242.
- Roman, L. J., & Kowalczykowski, S. C. (1989) *Biochemistry* 28, 2873–2881.
- Scott, J. F., Eisenberg, S., Bertsch, L. L., & Kornberg, A. (1977) *Proc. Natl. Acad. Sci. U.S.A.* 74, 193–197.
- Wong, I., & Lohman, T. M. (1992) *Science* 256, 350–355.
- Wong, I., Chao, K. L., Bujalowski, W., & Lohman, T. M. (1992) *J. Biol. Chem.* 267, 7596–7610.
- Wong, I., Amaratunga, M., & Lohman, T. M. (1993) *J. Biol. Chem.* 268, 20386–20391.
- Yarranton, G. T., & Gefter, M. L. (1979) *Proc. Natl. Acad. Sci. U.S.A.* 76, 1658–1662.
- Young, M. C., Kuhl, S. B., & von Hippel, P. H. (1994a) *J. Mol. Biol.* 235, 1436–1446.
- Young, M. C., Schultz, D. E., Ring, D., & von Hippel, P. H. (1994b) *J. Mol. Biol.* 235, 1447–1458.
- Zimmerle, C. T., & Frieden, C. (1989) *Biochem. J.* 258, 381–387.

BI952959I